Inorganic Chemistry

pubs.acs.org/IC

Communication

Selective Reduction of Niobium(V) Species to Promote Molecular Niobium/Tantalum Separation

Maxwell H. Furigay, Subhajyoti Chaudhuri, Sean M. Deresh, Alexander B. Weberg, Pragati Pandey, Patrick J. Carroll, George C. Schatz,* and Eric J. Schelter*

Cite This: *Inorg. Chem.* 2022, 61, 23−27

Read Online

ACCESS | Metrics & More | Article Recommendations | Supporting Information

ABSTRACT: The critical metals niobium (Nb) and tantalum (Ta) coexist in mineral sources, requiring a separation step to purify the elements from one another. The industrial separation process by solvent extraction uses stoichiometric hydrofluoric acid to manifest differences in the speciation of these otherwise chemically similar elements. The identification of alternative methods to separate Nb/Ta is desirable for fluoride waste reduction. In pursuit of this goal, the novel complexes $[Na(CH_3CN)_3(Et_2O)][M((S)\text{-}BINOLate)_3]$ [M = Nb (**1-Nb**), Ta (**1-Ta**)] were synthesized and characterized. In electrochemical studies, a reduction event at the potential −2.04 V versus ferrocene/ferrocenium was observed for **1-Nb**, whereas **1-Ta** exhibited no metal-based waves in the electrochemical window. In addition to the inherent 4d/5d orbital energy differences between Nb/Ta, density functional theory calculations suggest a larger degree of π donation from the ligands to the metal cation in **1-Ta** compared to **1-Nb**, destabilizing the lowest unoccupied molecular orbital. This phenomenon contributes to a calculated reduction potential difference of ca. 0.75 V, allowing for the selective reduction of **1-Nb** and separation of the reduction product through leaching with diethyl ether for a separation factor of 6 ± 2.

The growing need for consumer electronics continues to spur production of associated raw materials. The demands for tantalum (Ta), which is used in capacitors, and its chemical twin, niobium (Nb), which is widely used in steel alloys,[1] have exploded over the last 20 years, with global production doubling for Ta and quadrupling for Nb since 2000. Nb prices have similarly doubled over this period as the construction of pipelines and aviation alloys increases.[2] Because of their importance in technology in combination with a lack of diversification of their supply chains, both metals have been classified as critical by the National Research Council, and Ta has been classified as a conflict metal.[3]

Nb and Ta are primarily sourced from the minerals columbite $[(Mn,Fe)][(Nb,Ta)O_6]$ (Nb_2O_5 = 38−80%) and tantalite $[(Mn,Fe)][(Nb,Ta)O_6]$ (Ta_2O_5 = 40−86%)[4] and are invariably found together in their mineral matrices. As such, a separation step is required to purify the two elements from one another. However, Nb and Ta exhibit fundamentally similar chemical properties, with essentially identical ionic radii,[5] reactivity, and hardness, making their separation challenging.[6,7] The current industrial separation process requires fluorination of the mixed-metal oxides using stoichiometric hydrofluoric acid (HF), with associated challenges of toxicity, corrosivity, safety, and cost, but affords separation factors, $S_{Nb/Ta}$,[8] of >3500.[9] Current efforts to develop fluoride-free separation techniques have been met with limited success.[10,11] Nete and co-workers demonstrated that, given a mixture of niobium/tantalum pentafluorides, Nb can be selectively precipitated from the aqueous mixture with the chelating agent *p*-phenylenediamine ($S_{Nb/Ta}$ = 100). However, the use of fluoride is still required in this protocol.[12] Notably, Nete and co-workers also demonstrated the use of ion-exchange chromatography with free base resins to deliver Nb/Ta separations, reporting separation factors, $S_{Nb/Ta}$,[8] between 9.5 and 11.5 using a phosphoric acid eluent in place of the typical fluoride environment.[13,14]

Given the interest for developing sustainable methods of Nb/Ta separations that reduce the use of fluoride, we considered the problem from a coordination chemistry perspective. Accordingly, we report the synthesis and characterization of isostructural anionic complexes $[Na(CH_3CN)_3(Et_2O)][M((S)\text{-}BINOLate)_3]$ [M = Nb (**1-Nb**), Ta (**1-Ta**)] and describe a novel electrochemical method for separating these molecular compounds ($S_{Nb/Ta}$ = 6 ± 2). Racemic tris(BINOLate) complexes, charge-balanced with ammonium counterions, were reported previously.[15] However, that report lacked structural and NMR characterization data. Herein, electrochemical studies on **1-M** reveal differences in the $M^{V/IV}$ redox potentials, which are rationalized through computational studies in the context of ligand−metal π interactions. Although the current work does not address fluoride-free beneficiation of columbite/tantalite, these results indicate that electrochemical separations of Nb/Ta mixtures can be realized with tailored chelating ligands, supported by computational design and assessment. The results are reminiscent of work from Wang and Stiefel, wherein olefins

Received: September 23, 2021
Published: December 20, 2021

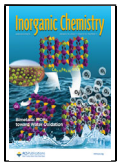

https://doi.org/10.1021/acs.inorgchem.1c02976
Inorg. Chem. 2022, 61, 23−27

were separated through the use of redox-active nickel complexes,[16] and previous work from our group, wherein rare-earth complexes were separated electrochemically.[17]

In pursuit of Nb/Ta complexes with strong donor ligands and potentially different electrochemical properties, the metal tris-(*S*)-(−)-1,1′-bis(2-naphthol) (BINOL)ate pinwheel complexes were synthesized through the addition of 3 equiv of (*S*)-BINOL to Nb/Ta$(NMe_2)_5$ and 1 equiv of sodium amide in benzene (Figure 1). Both complexes formed with sodium

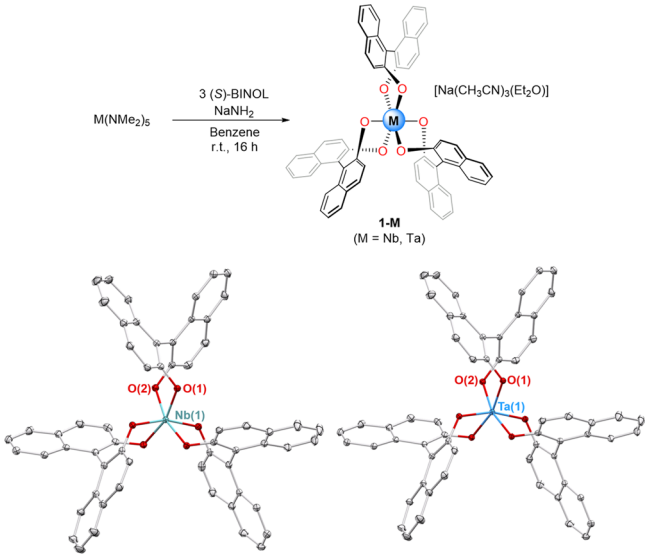

Figure 1. (Top) **1-M** synthetic scheme. (Bottom) Solid-state structures of **1-M**. Thermal ellipsoids are depicted at 50% probability, and counterions and hydrogen atoms are omitted for clarity.

counterions and were recrystallized through the vapor diffusion of diethyl ether (Et_2O) into acetonitrile (CH_3CN) solutions to form X-ray-quality crystals in 50−80% yield (Figure 1). Elucidation of the solid-state structures for **1-M** via X-ray crystallography indicated six-coordinate geometries at the metal cations and no significant differences in the bond lengths or angles between **1-Nb** and **1-Ta**. Both structures display C_3-symmetric geometries, and the Nb−O [1.977(3) and 1.976(3) Å] and Ta−O [1.974(3) and 1.975(3) Å] bond lengths (per asymmetric unit) are consistent with Nb/Ta in the 5+ oxidation state.[18]

Density functional theory (DFT) geometry optimizations were performed on **1-M** (B3LYP[19]/Def2-SVP[20]) and closely reproduced their experimentally determined bond lengths and angles, *vide supra* [see the Supporting Information (SI) for details]. These compounds display different chemical shifts in their respective ^{1}H NMR spectra (by ca. 0.05 ppm), allowing for the use of NMR spectroscopy as a means of differentiation (Figure S10).

To further characterize **1-M** and investigate differences between the two complexes, ultraviolet−visible (UV−vis) spectra were collected (Figure S6, solid traces). The UV−vis spectra show similar wavelengths of maximum absorption for **1-M** (λ_{max} = 231 nm), with **1-Ta** absorbing more strongly in the UV region. Time-dependent density functional theory (TD-DFT) calculations on **1-M** (B3LYP/Def2-SVP) were performed, providing spectra that qualitatively reproduced the experimental spectra of **1-M** (Figure S6, dashed traces). The two lowest-energy states calculated for **1-M** are composed primarily of highest occupied molecular orbital (HOMO)−lowest unoccupied molecular orbital (LUMO) and HOMO−LUMO+1 transitions (55−68% composition; see the SI for details). A difference in the energies of these states was predicted, with features corresponding to **1-Nb** (2.872 and 1.904 eV) calculated to be red-shifted compared to those of **1-Ta** (3.390 and 3.437 eV). Because of the use of the enantiopure (*S*)-BINOLate proligands and in contrast to the complexes reported by Andrä,[15] **1-M** are enantiopure complexes, and circular dichroism spectroscopy was employed to characterize their chiroptical properties (see the SI for details).

Electrochemical studies were undertaken to further assess the electronic structures of **1-M** and to identify the differences in their associated electron-transfer processes that could be used to develop **1-Nb**/**1-Ta** separations. Cyclic voltammograms (CVs) of **1-M** display irreversible oxidation features between 0.5 and 0.8 V versus ferrocene/ferrocenium (Fc/Fc^+), which, given the 5+ metal oxidation states, must correspond to BINOLate-based oxidation events (Figure 2A,B). These ligand-based oxidations are shifted anodically by ca. 0.13 V for **1-Ta** compared to **1-Nb**. The CV for **1-Nb** was found to display a reversible redox wave ($E_{1/2}$ = −2.04 V versus Fc/Fc^+) that we assign as the $Nb^{V/IV}$ redox couple. This value is consistent with values of −1.87 to −1.97 V versus Fc/Fc^+ reported for $Nb(OAr)_5$ (OAr = 4-Me-ArO, 3,5-Me_2-ArO, 2,6-Me_2-OAr) by Rothwell and co-workers.[21] A reversible metal-based reduction feature was not observed in the CV of **1-Ta** in the electrochemical window. Owing to 4d versus 5d orbital energy differences, Nb^V complexes reportedly exhibit more thermodynamically accessible $Nb^{V/IV}$ redox couples than their

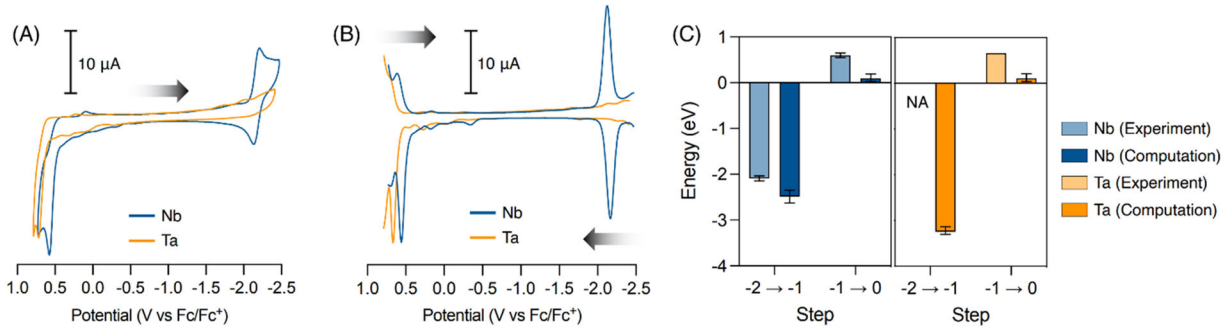

Figure 2. (A) CVs and (B) square-wave plots of **1-M** (see the SI for details). (C) Calculated and experimental redox potentials of **1-M** (error associated with the experimental **1-Ta** oxidation event = 0.5 μV).

https://doi.org/10.1021/acs.inorgchem.1c02976
Inorg. Chem. 2022, 61, 23−27

isostructural Ta^{V} congeners, and the chemistry of low-valent Nb is more developed.[22,23]

To probe the nature of these electron-transfer events, DFT geometry optimizations were performed on the singly oxidized and reduced forms of **1-M** ($[\mathbf{1\text{-}M}]^{+}$ and $[\mathbf{1\text{-}M}]^{-}$). These calculations corroborated the assignments postulated above and closely reproduced the experimentally determined redox potentials (Figure 2C). Of note, the putative $Ta^{V/IV}$ redox couple for **1-Ta** is predicted to occur at −3.24 V versus Fc/Fc^{+}, which is cathodically shifted by 0.75 V from the $Nb^{V/IV}$ couple calculated for **1-Nb** (−2.49 V vs Fc/Fc^{+}). Given the close agreement between the calculation and experiment for the experimentally observed BINOLate and $Nb^{V/VI}$ redox couples, the predicted potential suggests a reasonable explanation for the absence of a reversible $Ta^{V/IV}$ feature in the experimental CV of **1-Ta**. Examination of the computed **1-M** valence manifolds revealed differences in the compositions of the LUMOs between the complexes (Figure 3A). The **1-Nb** LUMO is best described as a metal d-orbital (58% d-orbital character), whereas that of **1-Ta** was calculated to contain less d-orbital contribution (22% d-orbital character) because of the larger ligand-based contribution to the LUMO. The difference in the orbital contribution between the complexes provides an added degree of π donation from the (*S*)-BINOLate ligands in **1-Ta** compared to **1-Nb**, which would be expected to destabilize the LUMO, making **1-Ta** more difficult to reduce (Figure 3B), in addition to inherent energy differences between the 4d/5d orbitals between these complexes. Indeed, upon a comparison of the quantitative (DFT-generated) valence orbital manifolds for **1-M**, substantial increases in the LUMO and LUMO+1 energies were observed for **1-Ta** compared to **1-Nb** (Figure 3C). This analysis is consistent with the TD-DFT-predicted HOMO−LUMO and HOMO−LUMO+1 transition energies being greater for **1-Ta** than for **1-Nb** (*vide supra*).

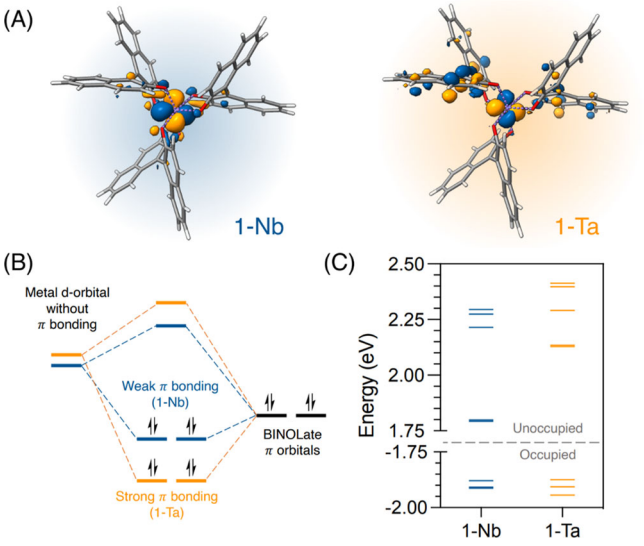

Figure 3. (A) LUMO orbitals (canonical) for **1-M** indicating the relative degrees of metal−ligand π interaction in **1-Nb**/**Ta** (isovalues = 0.04). (B) Qualitative MO diagram describing the impact of ligand π donation on **1-M** valence manifolds. (C) Quantitative (DFT-derived) **1-M** MO diagram depicting HOMO−HOMO−2 and LUMO−LUMO+4 orbitals.

The difference in the $M^{V/IV}$ redox couples for **1-Ta** versus **1-Nb** provides an exploitable property for the development of proof-of-concept chemical separations of the two complexes. Bis(pentamethylcyclopentadienyl)cobalt $[(C_5Me_5)_2Co]$ was selected as a reducing agent for effecting the selective reduction of **1-Nb** because its redox couple ($E_{1/2}$ = −1.91 V vs Fc/Fc^{+} in CH_3CN) makes it unlikely to reduce **1-Ta**. Accordingly, a homogenized mixture of **1-Ta** and **1-Nb** was treated with 10 equiv of $(C_5Me_5)_2Co$ in CH_3CN (Figure 4).

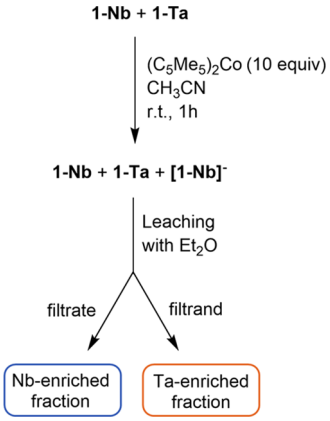

Figure 4. Nb/Ta separation flowsheet ($S_{Nb/Ta}$ = 6 ± 2).

An excess of reductant was necessary to favor $[\mathbf{1\text{-}Nb}]^{-}$ formation because of the similarity in the relevant redox couple of **1-Nb** versus $(C_5Me_5)_2Co$. After 1 h, volatile materials were removed under reduced pressure, and the reduction product(s) and unreacted $(C_5Me_5)_2Co$ were extracted from the resulting solid residue with Et_2O, leaving insoluble **1-M** behind (Figure 4). Analyzing the resulting residues using inductively coupled plasma-optical emission spectroscopy (ICP-OES) analysis (corroborated by NMR spectroscopy; see the SI for details) indicated that the insoluble solid was enriched in Ta (enrichment factor = 1.5 ± 0.1[8]), while the Et_2O extract was significantly enriched in Nb (enrichment factor = 4 ± 0.8). These enrichments are consistent with **1-Nb** being preferentially reduced over **1-Ta** to form a putative, reduction product $[\mathbf{(C_5Me_5)_2Co}][\mathbf{1\text{-}Nb}]$ and results in a modest separation factor, $S_{Nb/Ta}$, of 6 ± 2.[8] This result is comparable to the nonfluoride separation process reported by Nete and co-workers ($S_{Nb/Ta}$ = 11.5).[8,14] Upon the treatment of CH_3CN solutions of **1-M** with water, the (*S*)-BINOL ligands were recovered in 96−97% analytically pure yields (see the SI for details), demonstrating a framework for ligand recycling.

In conclusion, we have identified substantial differences in the redox properties of Nb/Ta-(*S*)-BINOLate complexes (**1-M**), allowing for the selective reduction of **1-Nb**. After reduction, the niobium product ($[\mathbf{(C_5Me_5)_2Co}][\mathbf{1\text{-}Nb}]$) was leached from unreacted **1-Ta**, resulting in a Nb-enriched filtrate and a Ta-enriched filtrand (separation factor = 6 ± 2). DFT calculations closely reproduced experimental spectra and electrochemical redox features for **1-M**, indicating that the ca. 0.75 V cathodic shift in the $M^{V/IV}$ redox couple of **1-Ta**, compared to **1-Nb**, is likely due to the inherent 4d/5d orbital energy differences, amplified by a greater degree of metal−ligand π bonding in **1-Ta**. These results demonstrate a novel molecular Nb/Ta separation process and provide a framework for alternative methods of the separation of these critical

https://doi.org/10.1021/acs.inorgchem.1c02976
Inorg. Chem. 2022, 61, 23−27

metals. The simple redox chemistry approach demonstrated here is expected to be applicable to a wide range of coordination compounds. Further work to expand the scope and efficacy of this strategy, through development of the role of π-bonded, chelating ligands, is underway to support the development of sustainable technologies based on these metals.

■ ASSOCIATED CONTENT

Supporting Information

The Supporting Information is available free of charge at https://pubs.acs.org/doi/10.1021/acs.inorgchem.1c02976.

Experimental section, NMR, IR, and UV−vis spectra, scan-rate-dependent electrochemistry data, circular dichroism spectra, ICP-OES data, sample calculations, and computational details (PDF)

Accession Codes

CCDC 2108600 and 2108601 contain the supplementary crystallographic data for this paper. These data can be obtained free of charge via www.ccdc.cam.ac.uk/data_request/cif, or by emailing data_request@ccdc.cam.ac.uk, or by contacting The Cambridge Crystallographic Data Centre, 12 Union Road, Cambridge CB2 1EZ, UK; fax: +44 1223 336033.

■ AUTHOR INFORMATION

Corresponding Authors

George C. Schatz − *Department of Chemistry and Graduate Program in Applied Physics, Northwestern University, Evanston, Illinois 60208, United States;* orcid.org/0000-0001-5837-4740; Email: g-schatz@northwestern.edu

Eric J. Schelter − *P. Roy and Diana T. Vagelos Laboratories, Department of Chemistry, University of Pennsylvania, Philadelphia, Pennsylvania 19104, United States;* orcid.org/0000-0002-8143-6206; Email: schelter@sas.upenn.edu

Authors

Maxwell H. Furigay − *P. Roy and Diana T. Vagelos Laboratories, Department of Chemistry, University of Pennsylvania, Philadelphia, Pennsylvania 19104, United States;* orcid.org/0000-0001-8643-7737

Subhajyoti Chaudhuri − *Department of Chemistry and Graduate Program in Applied Physics, Northwestern University, Evanston, Illinois 60208, United States;* orcid.org/0000-0001-8297-1123

Sean M. Deresh − *P. Roy and Diana T. Vagelos Laboratories, Department of Chemistry, University of Pennsylvania, Philadelphia, Pennsylvania 19104, United States;* orcid.org/0000-0003-2541-7841

Alexander B. Weberg − *P. Roy and Diana T. Vagelos Laboratories, Department of Chemistry, University of Pennsylvania, Philadelphia, Pennsylvania 19104, United States;* orcid.org/0000-0001-8421-9760

Pragati Pandey − *P. Roy and Diana T. Vagelos Laboratories, Department of Chemistry, University of Pennsylvania, Philadelphia, Pennsylvania 19104, United States;* orcid.org/0000-0003-0032-7364

Patrick J. Carroll − *P. Roy and Diana T. Vagelos Laboratories, Department of Chemistry, University of Pennsylvania, Philadelphia, Pennsylvania 19104, United States;* orcid.org/0000-0002-8142-7211

Complete contact information is available at: https://pubs.acs.org/10.1021/acs.inorgchem.1c02976

Notes

The authors declare no competing financial interest.

■ ACKNOWLEDGMENTS

The authors thank the Center for Sustainable Separations of Metals, an National Science Foundation Center for Chemical Innovation (Award CHE-1925708), for support of this work. S.M.D. thanks the Vagelos Integrated Program in Energy Research for support. We also thank the University of Pennsylvania and Northwestern University for support.

■ REFERENCES

(1) Linnen, R.; Trueman, D. L.; Burt, R. Tantalum and Niobium. In *Critical Metals Handbook*; Gunn, G.; Ed.; British Geological Survey: Nottingham, U.K., 2014; pp 361−382.

(2) Mackay, D. A. R.; Simandl, G. J. Geology, market and supply chain of niobium and tantalum—a review. *Miner. Deposita* **2014**, *49*, 1025−1047.

(3) Mancheri, N. A.; Sprecher, B.; Deetman, S.; Young, S. B.; Bleischwitz, R.; Dong, L.; Kleijn, R.; Tukker, A. Resilience in the tantalum supply chain. *Resour., Conserv. Recycl.* **2018**, *129*, 56−69.

(4) Agulyanksy, A. Fluorine Chemistry in the Processing of Tantalum and Niobium. In *The Chemistry of Tantalum and Niobium Fluoride Compounds*; Elsevier: San Diego, CA, 2004; pp 253−338.

(5) Shannon, R. D. Revised effective ionic radii and systematic studies of interatomic distances in halides and chalcogenides. *Acta Crystallogr., Sect. A: Cryst. Phys., Diffr., Theor. Gen. Crystallogr.* **1976**, *A32*, 751−767.

(6) Schultz, K. J.; Piatak, N. M.; Papp, F. J. Niobium and Tantalum. In *Critical Mineral Resources of the United States*; Schulz, K. J., DeYoung, J. H., Jr., Seal, R. R., II, Bradley, D. C., Eds.; United States Geological Survey: Reston, VA, 2017; pp M1−M31.

(7) Nete, M.; Purcell, W.; Nel, J. T. Hydrometallurgical Separation of Niobium and Tantalum: A Fundamental Approach. *JOM* **2016**, *68*, 556−566.

(8) The separation factor, $S_{Nb/Ta}$, refers to the product of the enrichment factors, $D_{Nb/Ta}$, for the two separation phases ($S_{Nb/Ta} = D_{Ta,Phase1} \times D_{Nb,Phase2}$). The enrichment factor refers to the molar ratio of elements in a given phase ($D_{Ta,Phase1} = \mu_{Ta,Phase1}/\mu_{Nb,Phase1}$. See the SI for sample calculations of both the separation and enrichment factors.

(9) Koerner, E. L., Jr.; Smutz, M.; Wilhelm, H. A. Separation of niobium and tantalum by liquid extraction. *Ames Laboratory ISC Technical Reports*, 1956; Vol. *151*.

(10) Agulyansky, A.; Agulyansky, L.; Travkin, V. F. Liquid−liquid extraction of tantalum with 2-octanol. *Chem. Eng. Process.* **2004**, *43*, 1231−1237.

(11) Zhu, Z.; Cheng, C. Y. Solvent extraction technology for the separation and purification of niobium and tantalum: A review. *Hydrometallurgy* **2011**, *107*, 1−12.

(12) Purcell, W.; Potgieter, H.; Nete, M.; Mnculwane, H. Possible methodology for niobium, tantalum and scandium separation in ferrocolumbite. *Miner. Eng.* **2018**, *119*, 57−66.

(13) Nete, M.; Purcell, W.; Nel, J. T. Separation of Niobium and Tantalum Pentafluoride by Selective Precipitation Using p-Phenylenediamine. *JOM* **2016**, *68*, 2817−2823.

(14) Nete, M.; Purcell, W.; Nel, J. T. Non-fluoride dissolution of tantalum and niobium oxides and their separation using ion exchange. *Hydrometallurgy* **2017**, *173*, 192−198.

(15) Andrä, K. Cyclische niob(V)- und tantal(V)säureester. *J. Less-Common Met.* **1969**, *17*, 297−303.

(16) Wang, K.; Stiefel, E. I. Toward Separation and Purification of Olefins Using Dithiolene Complexes: An Electrochemical Approach. *Science* **2001**, *291*, 106−109.

(17) Fang, H.; Cole, B. E.; Qiao, Y.; Bogart, J. A.; Cheisson, T.; Manor, B. C.; Carroll, P. J.; Schelter, E. J. Electro-kinetic Separation of Rare Earth Elements Using a Redox-Active Ligand. *Angew. Chem., Int. Ed.* **2017**, *56*, 13450−13454.
(18) Stavila, V.; Thurston, J. H.; Whitmire, K. H. Selective Arylation Reactions of Bismuth−Transition Metal Salicylate Complexes. *Inorg. Chem.* **2009**, *48*, 6945−6951.
(19) Becke, A. D. Density-functional thermochemistry. III. The role of exact exchange. *J. Chem. Phys.* **1993**, *98*, 5648−5652.
(20) Weigend, F.; Ahlrichs, R. Balanced basis sets of split valence, triple zeta valence and quadruple zeta valence quality for H to Rn: Design and assessment of accuracy. *Phys. Chem. Chem. Phys.* **2005**, *7*, 3297−3305.
(21) Coffindaffer, T. W.; Steffy, B. D.; Rothwell, I. P.; Folting, K.; Huffman, J. C.; Streib, W. E. Synthesis, Structure, and Bonding of Mononuclear Aryloxide Derivatives of Niobium in Oxidation States + 5, + 3, + 2, and + 1. *J. Am. Chem. Soc.* **1989**, *111*, 4742−4749.
(22) Parkin, G. Classification of Organotransition Metal Compounds. In *Comprehensive Organometallic Chemistry*, 3rd ed.; Mingos, D. M. P., Crabtree, R. H., Eds.; Elsevier: Oxford, U.K., 2007; Vol. *1*; pp 1−54.
(23) Beaumier, E. P.; Pearce, A. J.; See, X. Y.; Tonks, I. A. Modern applications of low-valent early transition metals in synthesis and catalysis. *Nat. Rev. Chem.* **2019**, *3*, 15−34.

https://doi.org/10.1021/acs.inorgchem.1c02976
Inorg. Chem. 2022, 61, 23−27